An Analysis of Moisture Structure and Rainfall for a Mei-Yu Regime in Taiwan

George Tai-Jen Chen

Department of Atmospheric Sciences
National Taiwan University
Taipei, Taiwan, Republic of China

Abstract

Moisture parameters and precipitation patterns are analyzed for a synoptic case of Mei-Yu in Taiwan during the period of June 10 through 15, 1975. The pre-existing rainfall systems as evidenced by radar echoes propagate southeastward with a wave period of 17 h and wavelength approximately 300 km over the Taiwan Strait. These systems tend to move toward right of the mean wind in 850-500 mb layer with an averaging deviation of 25°. As they move over the Taiwan Island, the local orographic effect and diuranl thermal control evidently play an important role in regulating both their intensities and spatial distributions. As a result, the mesoscale convective rainfalls have the peak time periods of 2.6, 3.5, and 7.1 h in northern Taiwan.

Results show that the low level southwesterlies, especially the Low Level Jet, tend to creat potential instability to the warm side of Mei-Yu Front. Continued large scale ascents then lead to the release of potential instability through organized mesoscale convective systems. The convection that is released produces the radar echoes and the cells of heavy precipitation.

Introduction

Climatological data show that the annual rainfall distribution in southeastern China possesses a relative maximum during the period of May and June. Continuous or intermittent precipitation mixed with frequent rainshowers and thunderstorms is the characteristic feature in this rainy season. A similar phenomenon is also found in Japan and in central and eastern China (i. e. along the Yangtze River) but in other months of a year (e. g. Ramage, 1971). This presummer rainy phenomnon is called "Mei-Yu" or "Plum Rain" in China and "Baiu" in Japan. Daily surface weather maps often indicate that a slow moving or stationary front extends from the vicinity of Japan southwestward into central or southern China in Mei-Yu season. Satellite pictures also reveal the nearly continuous cloud band along the front. This is often termed as a Mei-Yu Front or a Baiu Front.

The temperature gradient of a Mei-Yu Front is much weaker than that of a polar front. However, a series of disturbances at different scales, ranging from hundreds to thousands kilometers, is frequently observed to propagate northeastward along this front (e. g. Matsumoto et al, 1970; Ninomiya and Akiyama, 1972). A maximum frequency of the cyclogenesis of the intermediate-scale disturbance in East Asia was found in May and June during the period of 1966-1970 (Nitta and Yamanoto, 1972). Ninomiya and Akiyama (1972,1973), using multi-radar composite echo maps and detailed surface analyses, showed that the echoes are organized into medium-scale (about 1000 km) echo clusters in the frontal zone to the east of a synoptic scale cyclone. A surface isallobaric low and cyclonic wind circulation was found within these developed medium-scale echo clusters. The above cited research works were mainly on various aspects of a Baiu Front and its associated disturbances in the vicinity of Japan. In comparison, a relatively small amount of works has been done on the similar phenomena in southeastern China. Therefore, a case of Mei-Yu system in Taiwan is chosen in this study.

In Taiwan, Mei-Yu season is referred roughly to a month period beginning on May 15. A careful inspection of hourly rainfalls during this period discloses that mesoscale convective systems of order 10-100 km would be embedded within the steady type large scale Mei-Yu rainfall system. As a result, a possible flash flood situation may arise from an intense rainfall if the ground was already wetted by a previous continuous rain. Thus, understanding of the structure of a mesoscale rain system is necessary for short range forecasts of precipitation from a practical consideration. Also, better understanding on such phenomenon is needed for a parameterization of the convective mesoscale effects in models of large scale circulation. A case of June 10 to 15, 1975 was chosen in this study because Taiwan was under a typical Mei-Yu regime. The main purpose of this paper is to reveal rainfall characteristics and the large scale moisture field in the vicinity of Mei-Yu Front.

Cases and Data

Since we are interested in the moisture field and rainfall associated with Mei-Yu in Taiwan, synoptic cases in southeastern China and the vicinity of Taiwan have been chosen. Weather maps at surface and mandatory levels as well as the NOAA-4 satellite pictures as provided by the Chinese Air Force Weather Central (CAFWC) were basic synoptic data available in searching of cases in months of May and June for 1973-1975. These data were examined to see if there was a typical Mei-Yu case, i. e. the existence of a nearly stationary front and cloud band in southeastern China and the vicinity of Taiwan. In addition, hourly rainfall observations as obtained from the Chinese Central Weather Bureau (CCWB) were used to identify the characteristic feature of continuous or intermittent rains.

Cases of a 6-day period from June 10 to 15, 1975 are chosen for study on the basis of a well-defined Mei-Yu regime in Taiwan and its vicinity In addition, all the available surface and radiosonde data are most complete during this period.

The area of interest is roughly bounded by 10°N and 55°N, 85°E and 150°E. It includes southeastern China and its vicinity, Mongolia, Korea, Japan, Indo-China and the Western Pacific. There are a total of 140 radiosonde and 39 pibal stations in the area. Both 0000GMT and 1200GMT data at radiosonde stations are available with few exceptions. Numerous surface and radiosonde data in the neighboring areas are also used to help the analyses. These data were provided by the CCWB on the coded form transmitted from Japan Meteorological Agency (JMA) through a communication satellite. Notice that only the mandatory level data are available for almost all the stations in mainland China.

Rainfall data were obtained from various organizations on Taiwan Island. Daily totals were reported by 530 stations, While hourly rainfall amounts were obtained from 100 stations. Of these 100 stations reporting hourly rainfall amounts, 21 are maintained by CCWB. This mesoscale raingage network permits areal resolution of precipitation systems. Radar (WSR-64, 10 cm) echo reports are available at 3-hour intervals at Kaoshiung station of CCWB. In addition, the NOAA-4 satellite pictures in both the infrared and visible channels, orignally obtained from U. S. Environmental Data Service, National Climatic Center, are available during this case period.

Synoptic Situations

In general, mean sea level (MSL) pressure patterns showed that there were five major systems within the map area. Mongolia High was situated in the vicinity of Mongolia and northern China. A ridge of Okhotsk High extended from the Sea of Okhotsk southwestward into central Eastern China. A zone of low pressure and a midlatitude front (Front M) were located between these two high pressure systems. Ridge of subtropical Pacific anticlyclone extended southwestward into southwestern Pacific. A semistationary frontal zone was located in the region to the southeast of Japan, extended southwestward and passed through Taiwan Island into southern China. This frontal system located between the Okhotsk and Pacific ridges, is the Mei-Yu Front of interest in this study.

The Mei-Yu Front appeares to move very slowly southward from northern to central Taiwan by June 11 (Fig. 1). Daily rainfall totals in excess of 200 mm were reported at 0100GMT, June 12 over parts of Taiwan along the western coast. The Mei-Yu

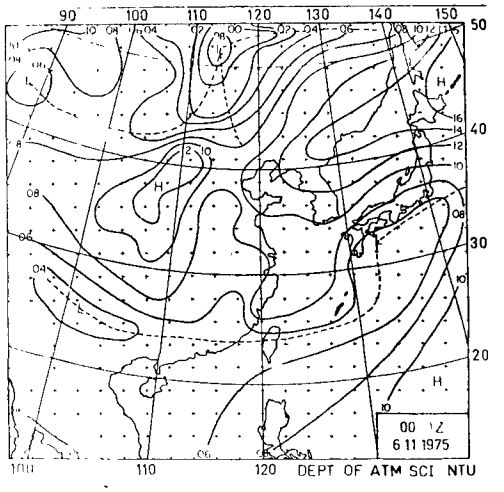

Fig. 1a

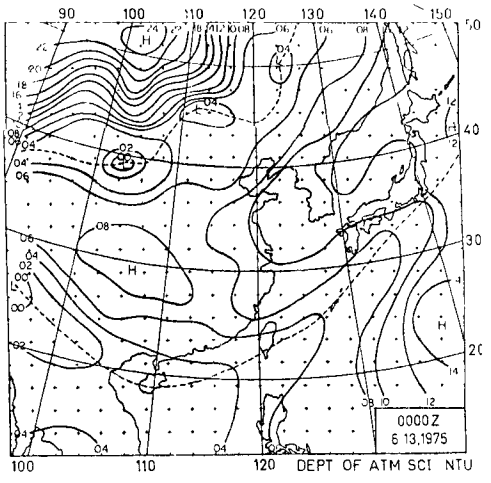

Fig. 1b

Fig. 1 Mean sea level pressure (solid) in mb and fronts (dashed) for (a) 11, 0000 GMT, (b) 13, 0000 GMT, June 1975.

Front continued to move slowly southeastward from central to southern Taiwan with a general easterly flow prevailed to the north of it by 0000GMT, June 13. The ridge to the northwest of Taiwan was weakening somewhat in the beginning and then regaining its intensity by the end of this period. Daily rainfall totals in excess of 100 mm were observed at 0100GMT, June 13 along the northwestern coast. The Mei-Yu Front then tended to stagnate in southern Taiwan, after 0000GMT on June 13, with an easterly surface wind component to the north and southerly wind component to the south of it. The short wave ridge to the northwest of Taiwan, while remained stationary, reached its maximum intensity at 1200GMT, June 14. It is an important feature in relation to the occurrence of fine weather in Taiwan

Fig. 2(a) shows 6-day rainfall totals in Taiwan from June 10 to 15. Moderate to heavy rains were generally observed to the west of the Central Mountain Range during this period. Some limited areas along the west coast received a total of more than 300 mm. On the other hand, light or no rain was usually observed to the east of the Central Mountain Range. A total of less than 20 mm rainfall was reported along the east coast. Smoothed topography is shown in Fig. 2(b) for reference.

The 850-mb charts are provided to show the lower tropospheric moisture distribution and to delineate areas of positive and negative moisture flux (Fig. 3). The major systems are quite similar in appearance to those on the surface. A remarkable shear line (also the trough line) is found to the north and northwest of the associated surface Mei-Yu Front. It moves south or southeastward slowly. Rather weak contour gradient is generally found in southeastern China and the East China Sea along shear line. southeastern China and the East China Sea along shear line. Westerlies to southwesterlies prevailed in the vicinity of Taiwan to the south of shear line from June 10 to 12. A closed low circulation was formed over Taiwan on June 13 and continued to exist on June 14. A nearly stationary closed low at 700 mb was located over the Sea of Japan with a slowly filling rate during the case period (not shown). A trough line extended from the low center southwestward passing through the area to the north of Taiwan into southwestern China. While this trough moved slowly southeastward to the northwest of Taiwan, westerly to southwesterly flow generally prevailed in the vicinity of Taiwan until the southerlies set in on June 15.

The synoptic situations on 500 mb show that a cut-off low at the Sea of Japan moves slowly southward then northeastward during the case period. A trough extends from this low center southwestward to the vicinity of Taiwan. The advection of

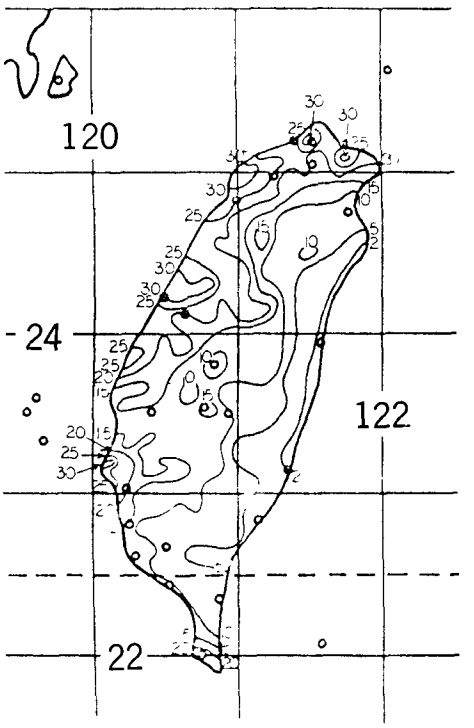

Fig. 2a

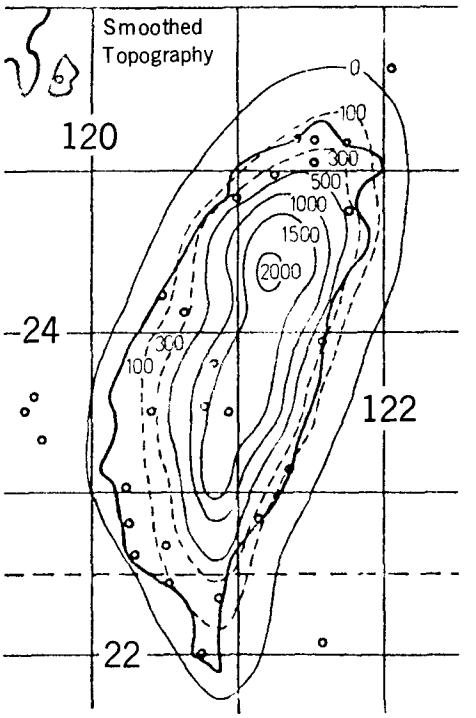

Fig. 2b

Fig. 2 (a) Total rainfalls (cm) in Taiwan for the 6-day period of June 10-15, 1975. (b) Smoothed topography (m).

cold air into the major trough and the existence of a secondary trough over North Korea on June 10 points to the intensification of the major trough (Fig. 4a). The trough intensifies and extends over Taiwan on June 12 (Fig. 4b) and weakens in later stage of the case period. The well-defined baroclinic zone is generally located to the north of 30°N latitude and reaches the maximum intensity on June 12 especially over central China, the East China Sea and the vicinity of Japan. A closed High is generally found over the South China Sea. Warm air was observed over central and southern China with the highest temperature of -2°C on both June 11 and 14. Between the Pacific ridge to the east and the closed High to the west, the trough region is usually found in the vicinity of Taiwan and the Philippines.

The NOAA-4 satellite pictures in infrared channel are shown in Fig. 5 for June 11 and 12. The brightness shows the temperature of blackbody radiation with the area of low temperature shown by the white area in the picture. Thus, the brightness in the picture indirectly indicates the thickness and height of the cloud. A continuous cloud band in association with the Mei-Yu Front is found extending from Japan southwestward into southeastern China. Thick cloud band is found to the north of Taiwan on June 10, over Taiwan on June 11 and 12, and to the south of Taiwan after June 13.

Vertical cross sections of wind speed and mixing ratio along 120°E at 1200GMT are shown in Fig. 6.

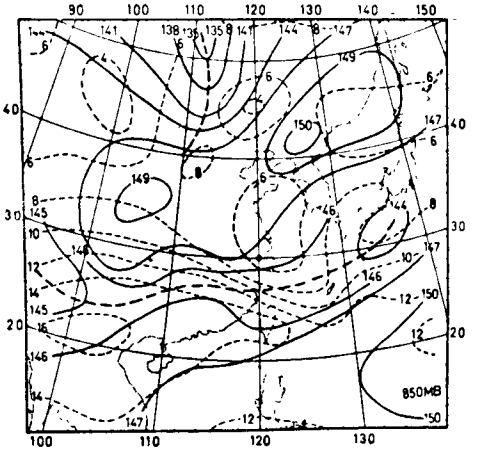

Fig. 3a

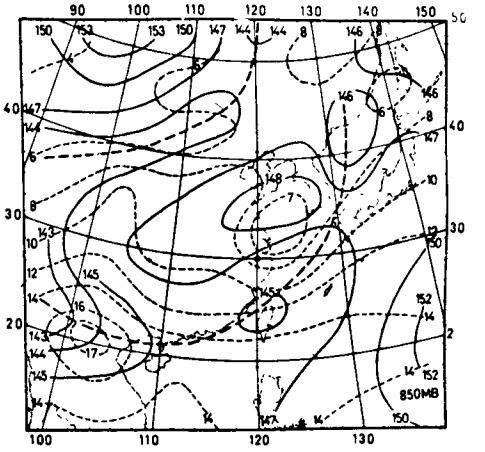

Fig. 3b

Fig. 3 Geopotential height (solid) in dam, mixing ratio (dashed) in g Kg^{-1} and troughs (or shear lines, heavy dashed) on 850 mb for (a) 11, 0000 GMT, (b) 13, 0000 GMT, June 1975

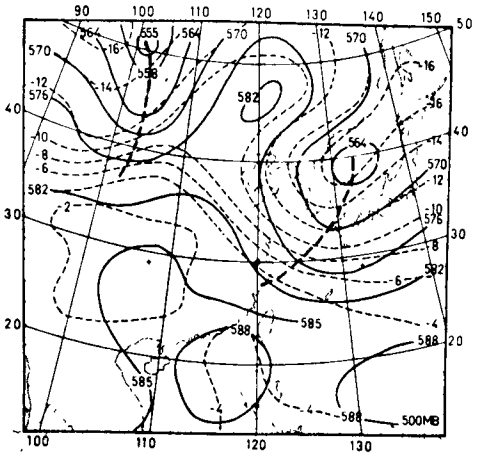

Fig. 4a

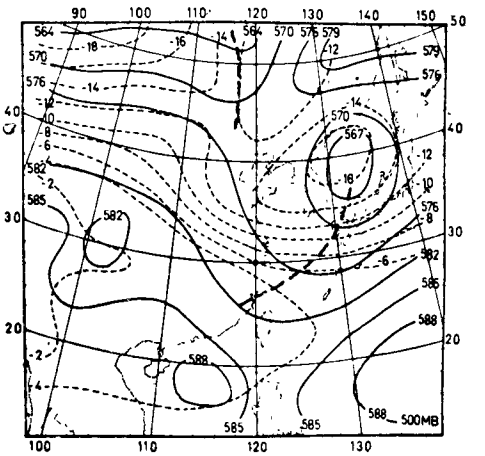

Fig. 4b

Fig. 4 Geopotential height (solid) in dam and temperature (dashed) in °C on 500 mb for (a) 10, 0000 GMT, (b) 12, 0000 GMT, June 1975.

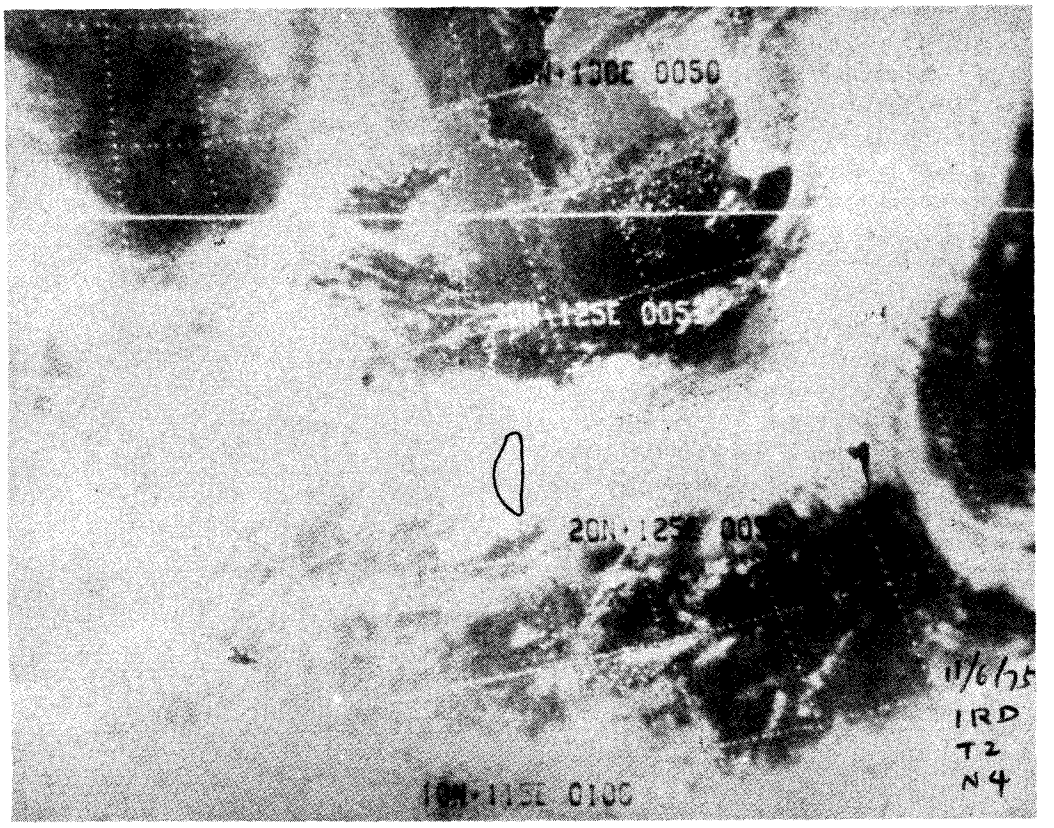

Fig. 5a

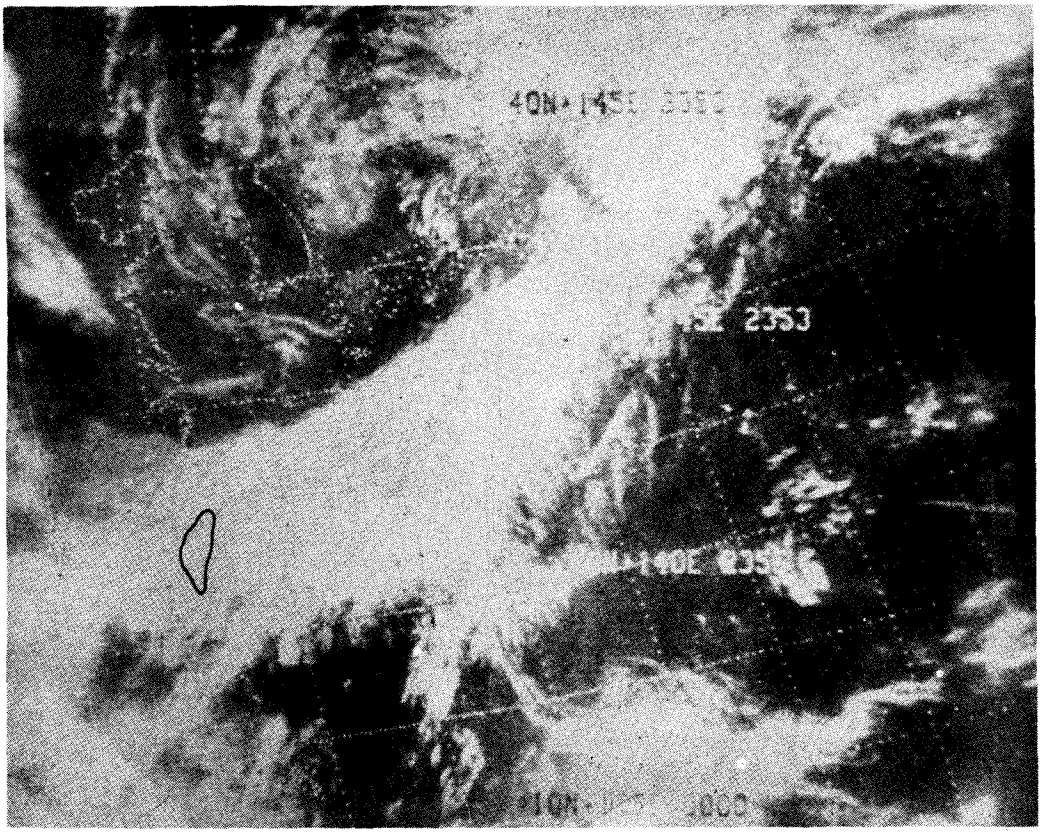

Fig. 5b

Fig. 5. NOAA-4 satellite pictures in infrared channel for (a) June 11, (b) June 12, 1975. Geography of Taiwan is shown by solid black curve.

for June 10 to 12. The low level jet stream (LLJ) is clearly indicated near 700 mb in the vicinity of Taiwan (near J=6) before June 12 but not in the later time period. Notice that the area of maximum moisture content coincides with the LLJ and the maximum gradient of mixing ratio is just to the north of the LLJ.

The LLJ core is observed near 600 mb at Taipei (Fig. 7(b)) on June 11,0000GMT, and near 700 mb at Makung (Fig. 8(b)) and Tungkong (Fig. 9(b)) 12 h later. A low level easterly jet of 13 m s^{-1} on 900 mb at 0000GMT, June 13 is observed at Taipei but not at the other two stations. The rainfall over northern Taiwan diminished after 0000GMT, June 13 as the easterly jet set in at Taipei at the same time. The boundary between the low level easterly

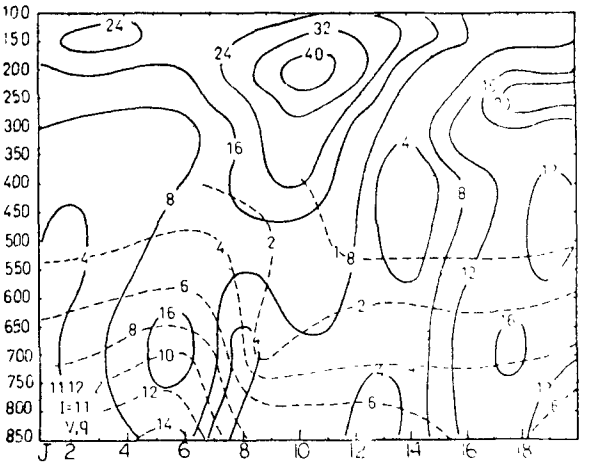

Fig. 6b

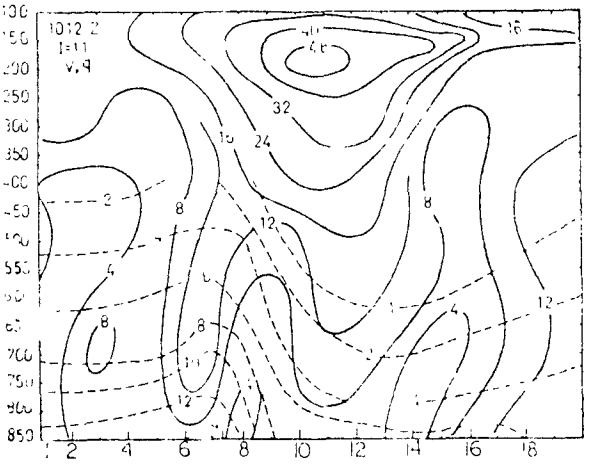

Fig. 6a

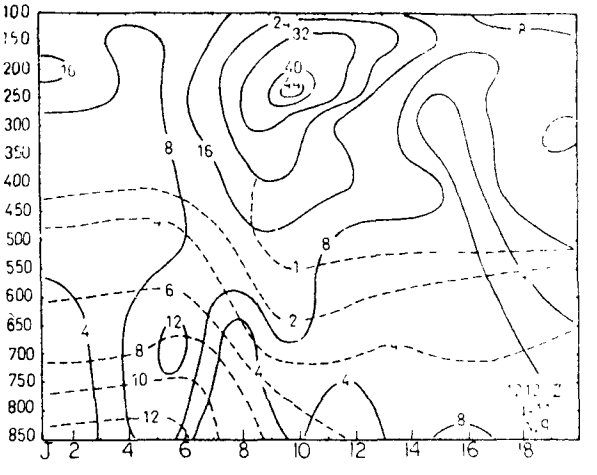

Fig. 6c

Fig. 6 Vertical cross sections of wind speed (solid) in m s^{-1} and mixing ratio (dashed) in g Kg^{-1} along 120°E (I=11) for (a) 10, 1200GMT, (b) 11, 1200 GMT, (c) 12, 1200 GMT, June 1975. J indices in increasing order are from south to north.

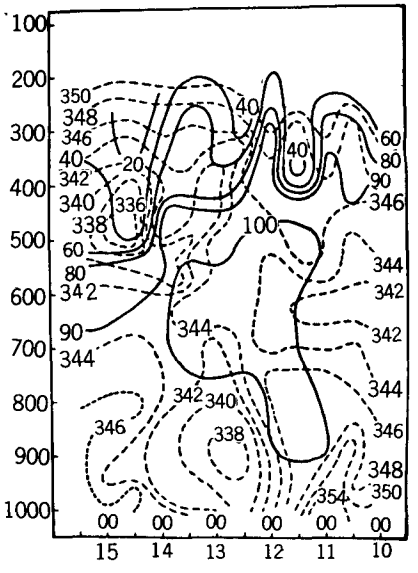

Fig. 7a

Fig. 7

Time sections at Taipei at 12-h intervals from June 10 through 15, 1975 for (a) relative humidity (solid, in %) and equivalent potential temperature (dashed, in °K), (b) wind speed in m s^{-1} and boundary (dashed) between easterlies (E) and westerlies (W).

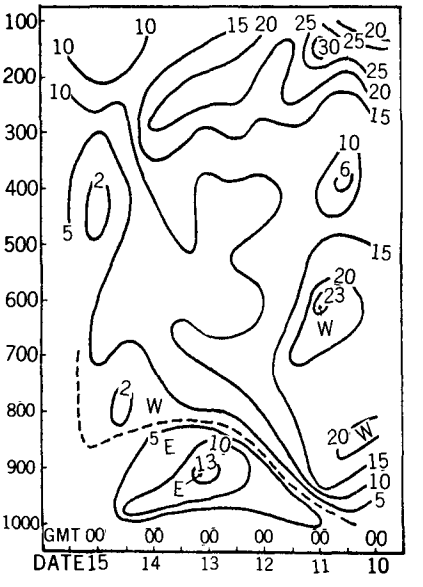

Fig. 7b

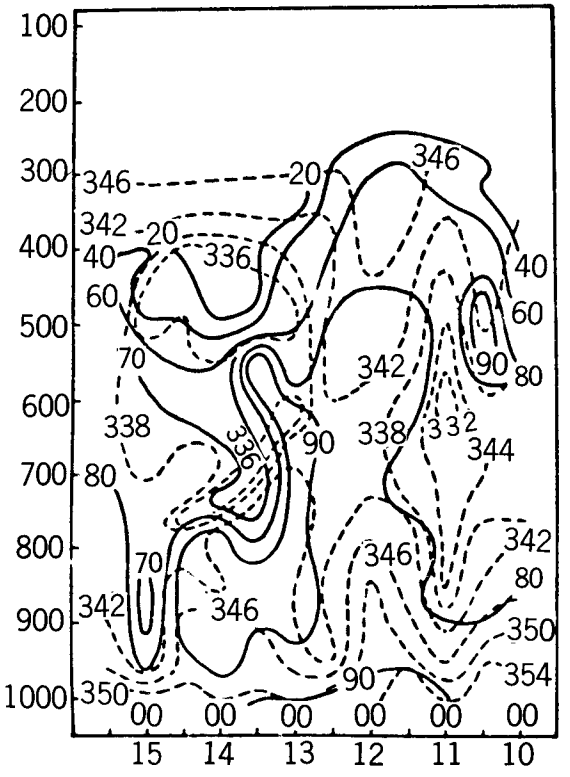

Fig. 8a

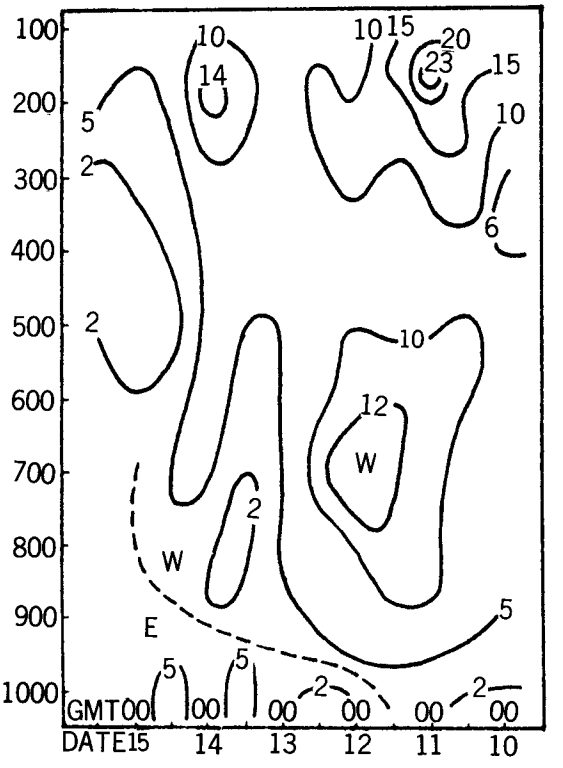

Fig 8b

Fig. 8 Same as Fig. 7, except at Makung.

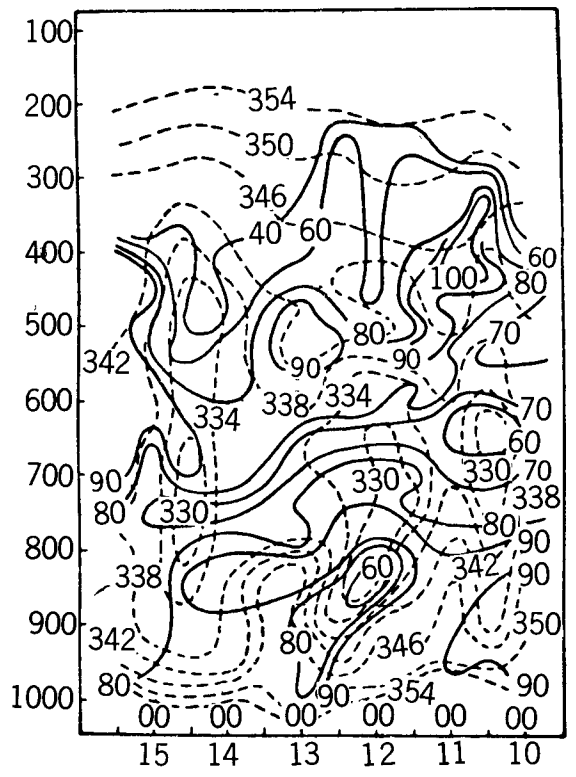

Fig. 9a

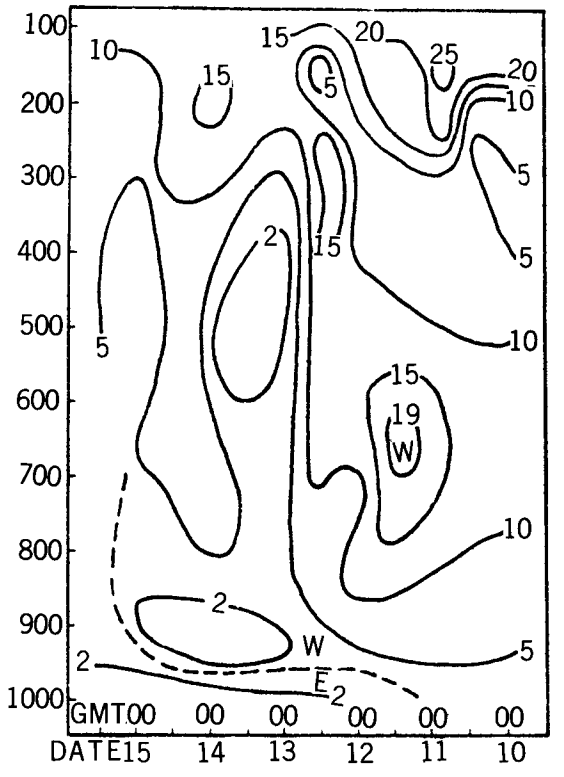

Fig. 9b

Fig. 9 Same as Fig. 7 except at Tungkong

and westerly wind regimes as indicated by a dashed line shows the passage of Mei-Yu Front. In view of the diurnal and local influences on the surface winds in this time of the year, time cross section analyses as well as surface maps (Fig. 1) indicate that the Mei-Yu Front passed through Taipei at 0000GMT, June 10, Makung at 1200GMT, June 11 and Tungkong at 0000GMT, June, 12.

Results

Moisture Field and Cloudiness

Patterns of mixing ratio at 850 mb (Fig. 3) shows that the maximum gradient is generally observed in the vicinity of the Mei-Yu trough. A maximum center is observed over northern Indo-China with the major axis extending eastward across southern Taiwan and the Bashi Channel, to the western Pacific before June 12. As a result, maximum flux of moisture is found to the south of Mei-Yu trough, especially in the vicinity of Taiwan. Mixing ratio over Taiwan decreased after June 12 as the trough moved southward over the area. A minimum center is observed over the East China Sea and its vicinity. The South China Sea was a comparatively less moist area during the case period.

Vertical cross sections of mixing ratio along 120°E are shown in Figs. 6(a) through 6(c) at 1200GMT from June 10 to 12. The maximum gradient is clearly seen over the East China Sea (J=7 to 10) and maximum value is found over Taiwan below 500 mb until June 12. Axis of minimum value generally tilts northward with height from the area just to the north of the maximum gradient. A region of relatively dry air is found directly under the influence of the upper level jet.

Time sections of relative humidity (RH) and equivalent potential temperature (θ_e) at three radiosonde stations in Taiwan are shown in Figs. 7(a), 8(a) and 9(a) at 12-h intervals from June 10, 0000GMT to 15, 1200GMT.

At Taipei, ninety percent RH generally prevails in the lower troposphere. Saturation is found between 900 mb and 500 mb in the period of June 11, 0000GMT to June 12, 0000GMT and between 750 mb and 500 mb in the period of June 12, 0000GMT to 14, 0000GMT. Cloud tops above 300 mb level are suggested by the RH of more than 90% before June 12. The distribution of equivalent potential temperature shows that the potential instability reaches a maximum value below 800 mb in the period of June 10, 1200GMT through 11, 1200GMT just prior to the time of occurrence of the maximum RH in middle troposphere. As the atmosphere between 900 mb and 600 mb changes on June 12, 0000GMT from the potentially unstable to the potentially stable condition, the thickness of the saturation layer tends to decrease. The easterly is associated with low θ_e and westerly with high θ_e.

At Makung, the layer of moist air (RH>80%) is confined below 900 mb level before June 11, 0000GMT, and extends to 450 mb between 11, 0000GMT and 13, 0000GMT, then decreases to 950 mb at 0000GMT on June 15. Maximum RH is found near the surface from 11, 0000GMT through 13, 1200GMT and also in the layer between 900 mb and 600 mb after 13, 0000GMT. The atmosphere is potentially unstable below 600 mb during the case period. The maximum potential instability is generally observed prior to the occurrence of maximum RH. The LLJ is associated with high θ_e.

At Tungkong, the moist air (RH>80%) is found in the layer below 750 mb level before June 14, 1200GMT except near 800 mb at 0000GMT of June 12. Another layer of moist air is located near 400 mb on June 10 and descends to near 600 mb on June 15. The potentially unstable atmosphere is generally found below 700 mb level. Again, the LLJ is associated with high θ_e.

Distributions of the RH and vertical velocity on 850,700 and 500 mb are shown in Figs. 10(a) through 10(f) at 0000GMT, June 11 and 12. The vertical velocity was computed by a kinematic method identical to that used in Chen (1976). At 850 mb, moist air (RH>80%) is found in the vicinity and to the south of Mei-Yu trough. An area of high RH in excess of 90% is observed over Taiwan and its vicinity where the maximum upward motion prevails. Dry air is usually found over the area between the Mei-Yu and mid-latitude troughs. At 700 mb, strong gradient of RH is generally observed across the Mei-Yu trough, especially over the East China Sea. A moist area of RH greater than 90% is generally observed in the vicinity of Taiwan and the area to the east. Saturated air is found to the east of Taiwan on June 12. Maximum upward motion of 2-3 $\mu b\ s^{-1}$ is observed over Taiwan and the vicinity. At 500 mb, the maximum gradient of RH is found over the East China Sea and the vicinity of Japan. Moist air of RH greater than 90% is found over the area to the east of Taiwan. Maximum upward motion in excess of 3-4 $\mu b\ s^{-1}$ is observed over the same area. Dry air of RH less than 10% is observed over eastern China and the East China Sea. Another area of relatively dry air is found over the South China Sea.

Vertical cross sections of θ_e and RH along 120°E are shown in Figs. 11(a) through 11(c). Moist air located to the north of Taiwan (J=6 to 8) at all levels on June 10 moves southward into the Bashi Channel (J=4 to 5) after June 12. Downward extension of the dry air over the East China Coast (J=8 to 11) is clearly indicated. On June 10, axis of maximum gradient of θ_e on 850 mb is found over the East China .Coast with a northward tilt with

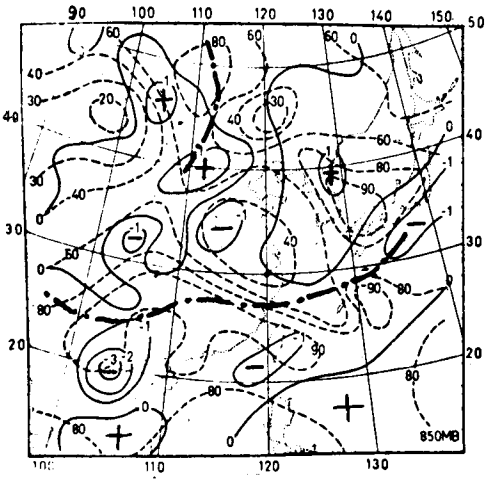

Fig. 10a

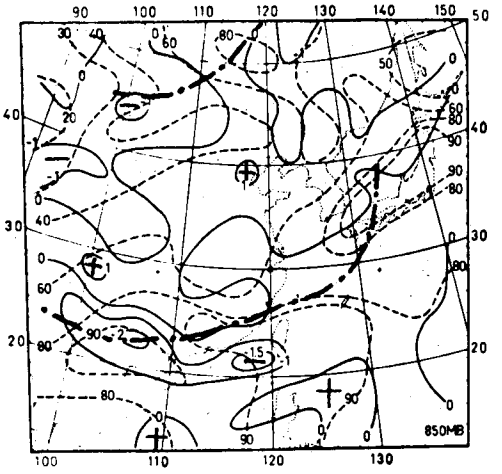

Fig. 10b

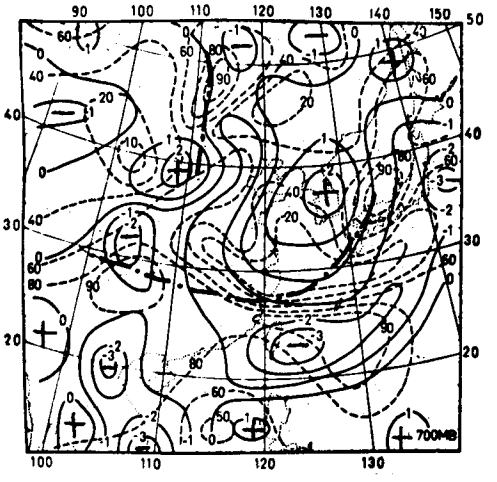

Fig. 10c

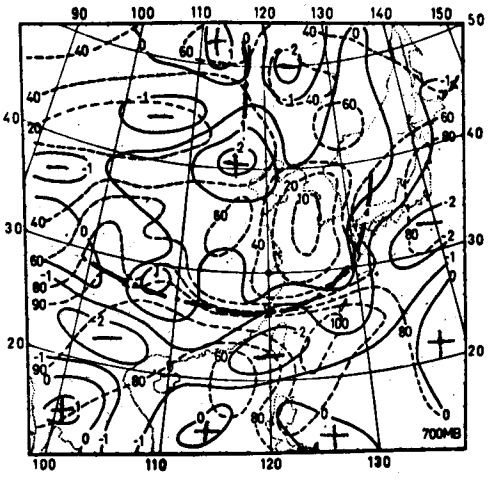

Fig. 10d

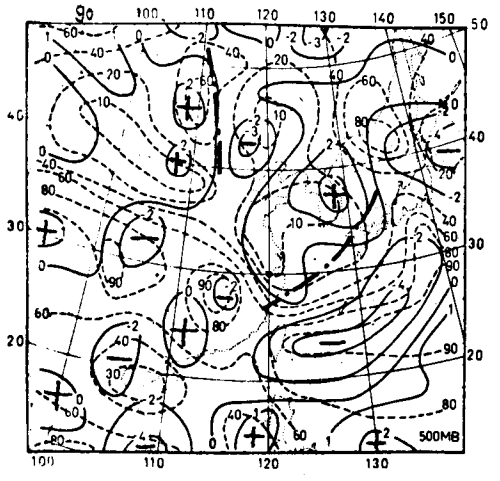

Fig. 10e

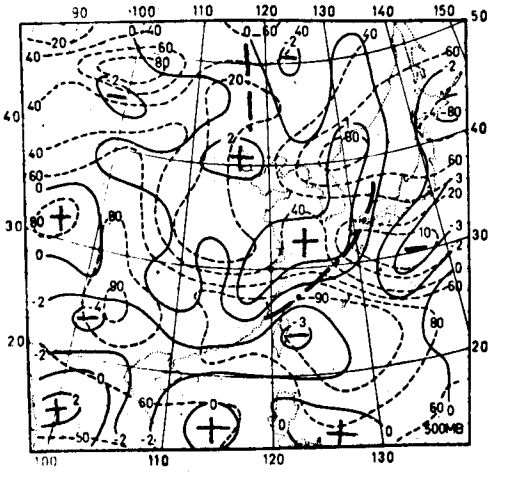

Fig. 10f

Fig. 10 Vertical velocity (solid) in μb s^{-1} and relative humidity (dashed) in % for (a) 11, 0000 GMT at 850 mb, (b) 12, 0000 GMT at 850 mb, (c) 11, 0000 GMT at 700 mb, (d) 12, 0000 GMT at 700 mb, (e) 11, 0000 GMT at 500 mb, (f) 12. 0000 GMT at 500 mb.

height. Maximum gradient of θ_e is found over Taiwan at 850 mb on June 12. Moist air to the south of maximum gradient of θ_e is generally found with potentially neutral or potentially unstable conditions. Note that the LLJ near 700 mb is associated with high θ_e (Figs. 6 and 11).

Distributions of total precipitable water in the layer from 850 mb to 400 mb at 0000GMT are shown in Fig. 12 for June 12 and 14. The maximum gradient is found from the area to the south of Japan to central China. A maximum center is found over southwestern China with moist tongue extending to the area north of Taiwan on June 10 and to the area south of Taiwan after June 14. A minimum center is observed over the East China Set and its vicinity. A reltively dry area is also found in the vicinity of the Philippines.

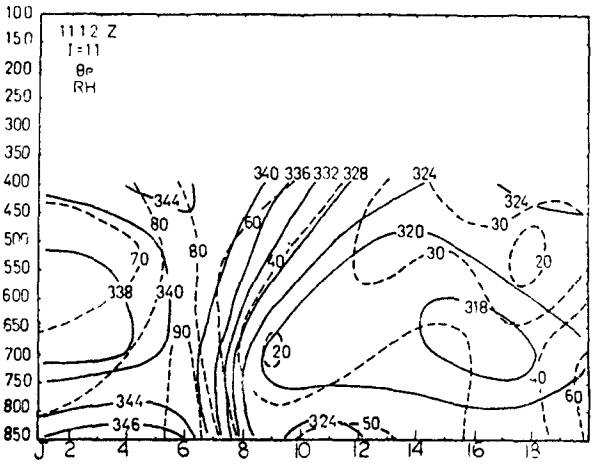

Fig. 11b

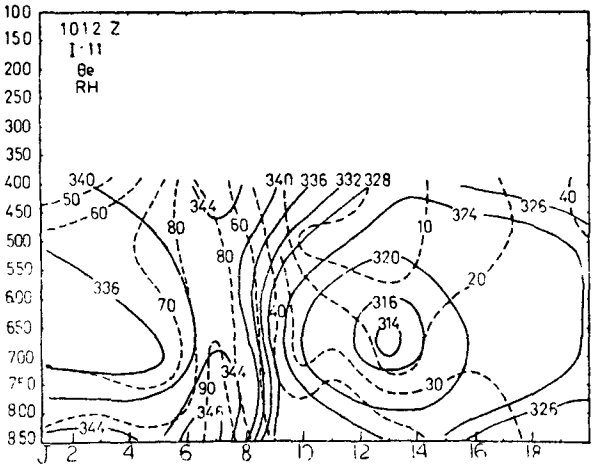

Fig. 11a

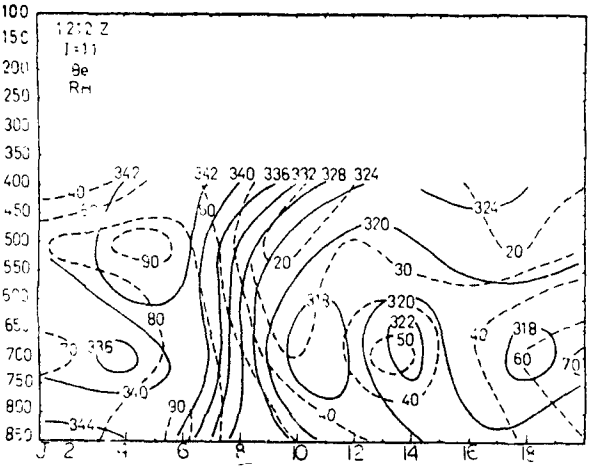

Fig. 11C

Fig. 11 Vertical cross sections of equivalent potential temperature (solid) in °K and relative humidity (dashed) in % along 120°E (I=11) for (a) 10, 1200 GMT, (b) 11, 1200 GMT, (c) 12, 1200 GMT, June 1975.

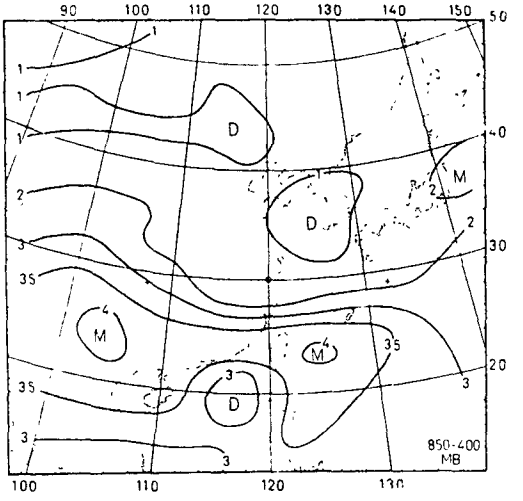

Fig. 12a

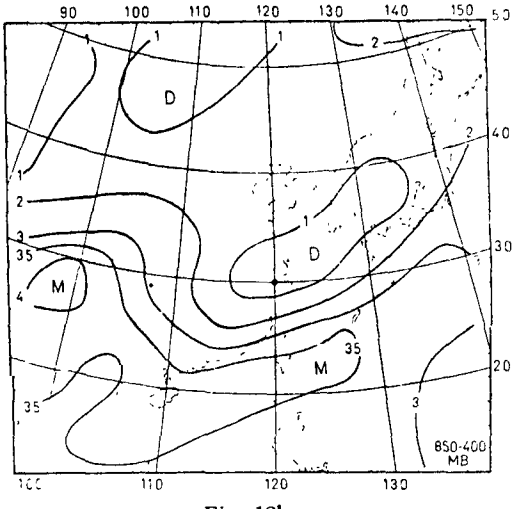

Fig. 12b

Fig. 12 Total precipitable water (in cm) between 850 mb and 400 mb for (a) 12, 0000 GMT, (b) 14, 0000 GMT, June 1975.

False color pictures of NOAA-4 IR channel, as shown in Fig. 5. are analyzed in Figs. 13(a) through 13(c). The thick cloud zone is found along and to the south of Mei-Yu Front on June 10. Thin cloud over central and southern Taiwan on June 10 coincides with the observed small amount of precipitation in the same area. Maximum rainfall observed on June 11 over Taiwan is also indicated by the thick cloud cover. The pre-existing rain system in the Mei-Yu cloud band, the northeastward transport of moisture into the Mei-Yu convergence zone, and the northward propagation of rain system in the later time period over the Bashi Channel are also seen in these pictures.

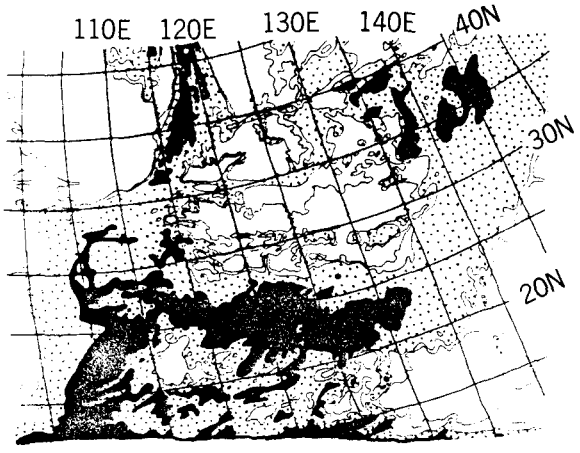

JUNE 11. 1975 NOAA-4 IR

Fig. 13b

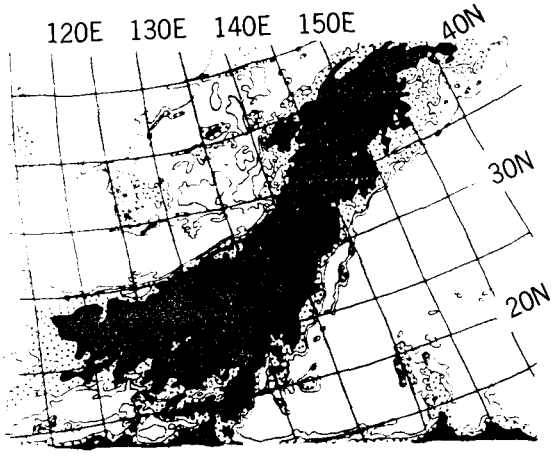

JUNE 10, 1975 NOAA-4 IR

Fig. 13a

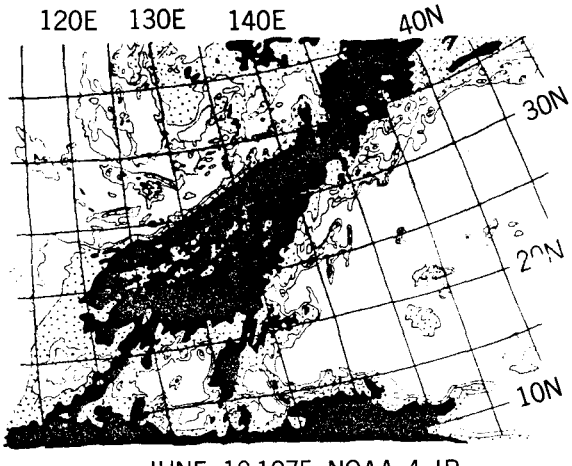

JUNE 12,1975 NOAA-4 IR

Fig. 13c

Fig. 13 False color analyses of NOAA-4 IR pictures for (a) June 10, (b) June 11, (c) June 12, 1975. Relative cloud thickness (and/or cloud height) are divided into three classes represented by dark, dotted, and open areas in a decreasing order of the relative thickness.

The distribution of 6-day mean cloudiness was obtained by averaging cloud amounts (in tenth unit) estimated from the NOAA-4 satellite pictures in visible channel on a 2.5x2.5 degree longitude-latitude grids. Maximum cloudiness of more than 8-tenth is found along a zone from the south of Japan, passing through Taiwan, to southeastern China. Minimum cloudiness of below 4-tenth is observed over the Yellow Sea and northern China as well as the South China Sea and western Pacific (Fig. 14). The maximum cloudiness zone is generally along the 1000 mb mean trough and minimum cloudiness was along the 1000 mb mean ridge. The mean cloudiness is found to have a rather good positive correlation with the mean relative humidity on 700 mb except in the lower latitudes. For example, the area of relative humidity in excess of 80% coincides with the area of mean cloudiness above 8-tenth and the area of relative humidity less than 40% is associated with the area of mean cloudiness below 4-tenth.

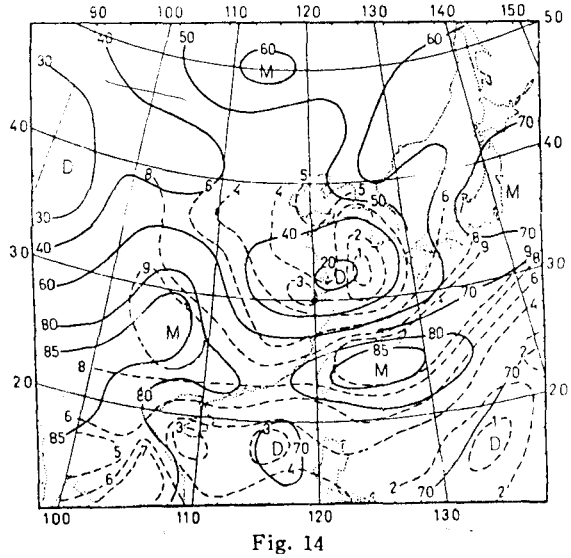

Fig. 14

Fig. 14 Mean relative humidity (solid, in %) at 700 mb and NOAA -4 mean cloudiness (dashed) for June 10-15, 1975. Moist (M) and dry (D) areas are indicated.

Surface Rainfall and Radar Observations

Daily rainfalls in association with the Mei-Yu Front in Taiwan are briefly discussed for the period from June 10, 0100GMT to 15, 0100GMT. On the first day, rainfall was mainly observed on northwestern Taiwan and the western slope of the Central Mountain Range. An area of precipitation greater than 50 mm was found along the northwestern coast. On the second day, the greatest amount of rainfall was observed over most of the area especially along the western coast. Some areas along the coast had rainfall in excess of 200 mm. The 20 mm isohyet was along the ridge of Central Mountain Range with the rainfall of less than 20 mm to the east side. On the third day, the rainfall amount was generally less than that of the previous day. Daily rainfall of greater than 100 mm was observed in the northern and the western coast of Taiwan. On the fourth day, a general decrease of rainfall to the northwest were observed. Again, the maximum rainfall was observed along the coast. A primary maximum rainfall of greater than 150 mm was found to the southwestern coast. On the fifth day, further decrease of rainfall was observed except on the mountain area and the southwestern slope.

For the purpose of this paper, rainfall during a 48-h period beginning at 0000LST, June 11 was chosen for more detailed analysis because of the existence of intense rainfall all over the Taiwan Island and the evident mesoscale convective systems during this time period. Six-hour rainfall patterns are shown in Figs. 15 and 16. Note that the LST is

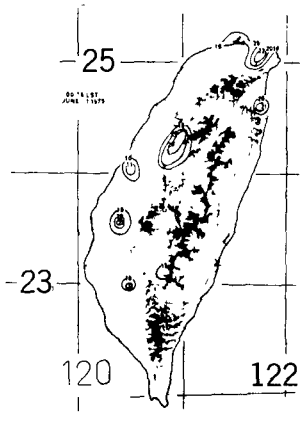

Fig. 15a

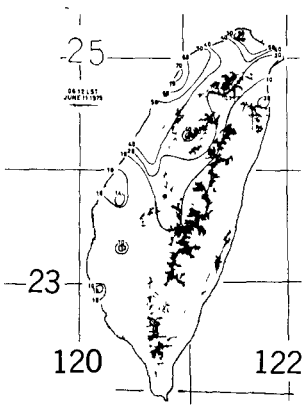

Fig. 15b

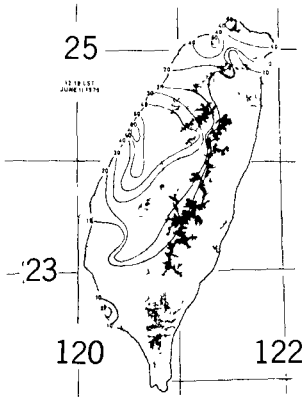

Fig. 15c

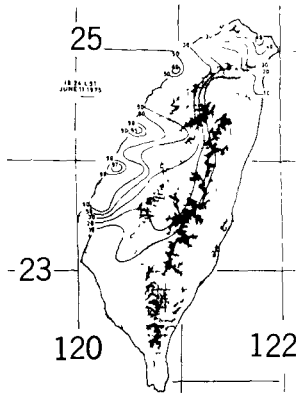

Fig. 15d

Fig. 15 Six-hour rainfall amounts (mm) in Taiwan for (a) 0000-0600 LST, (b) 0600-1200 LST, (c) 1200-1800 LST, (d) 1800-2400 LST, June 11, 1975.

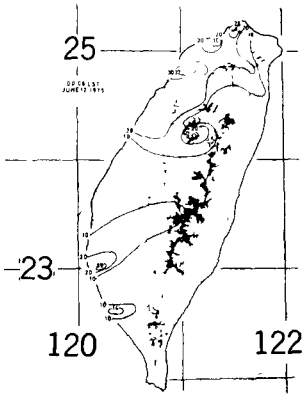

Fig. 16a

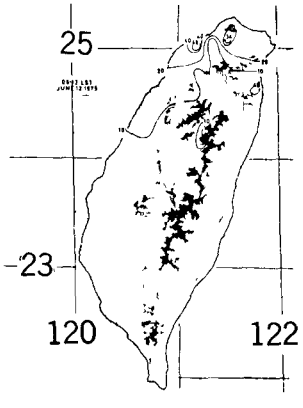

Fig. 16b

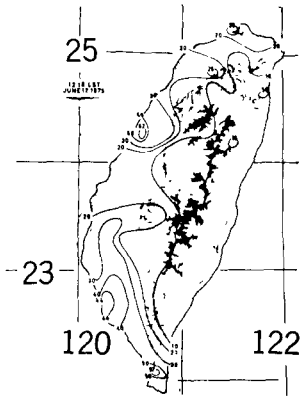

Fig. 16c

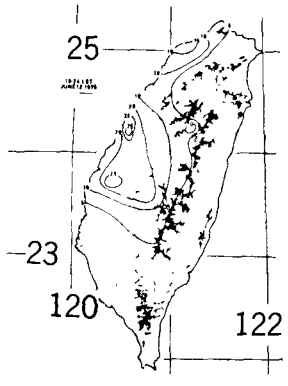

Fig. 16d

Fig. 16 Six-hour rainfall amounts (mm) in Taiwan for (a) 0000-0600 LST, (b) 0600-1200 LST, (c) 1200-1800 LST, (d) 1800-2400 LST, June 12, 1975.

8 h ahead of the GMT. During the first 6 hour of June 11, some areas along the coast and the western slope of the Central Mountain Range had rainfall of 20 mm or greater. A great amount of rain fell on northwestern Taiwan during the next 6 hour. Maximum rainfall of greater than 70 mm was observed on the northwestern coast. This center of maximum rainfall moved southward along the coast and had maximum values greater than 80 mm and 95 mm for the following and last 6 h period, respectively, on June 11. Evidently, well-defined spatial and temporal continuity was exhibited by the maximum rainfall region as it moved southward along the coast between 0600LST and 2400LST. On June 12, rainfall was mainly observed on the northwestern and southwestern Taiwan during the first 6 hour. For

the next 6 hour, the rainfall was mostly confined to the northwest with a maximum of greater than 40 mm. The maximum rainfall center tended to move southward along the west coast for the next 12 h period.

Hourly rainfall patterns from 1000LST to 1400LST on June 11 are shown in Fig. 17. A local maximum was observed to the north of 24°N near Taichung with the hourly maximum of 10, 32, 11, and 26 mm during this 4 h period In general, the rainfall was mainly observed to the west of the Central Mountain Range especially along the coast with a general trend of southward movement of the main precipitation system.

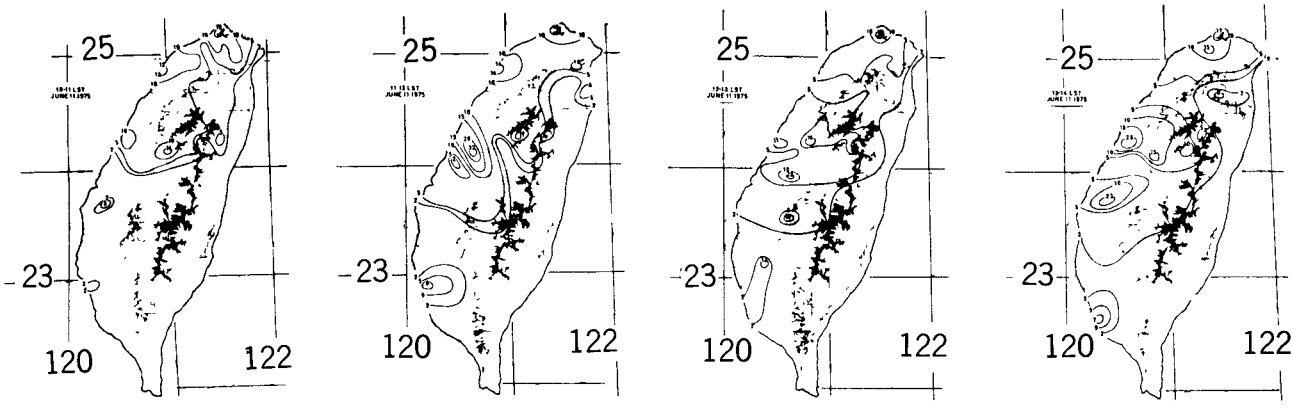

Fig 17a Fig. 17b Fig. 17c Fig. 17d

Fig. 17 Hourly rainfall (mm) in Taiwan on June 11, 1975 for (a) 1000-1100 LST, (b) 1100-1200 LST, (c) 1200-1300 LST, (d) 1300-1400 LST,

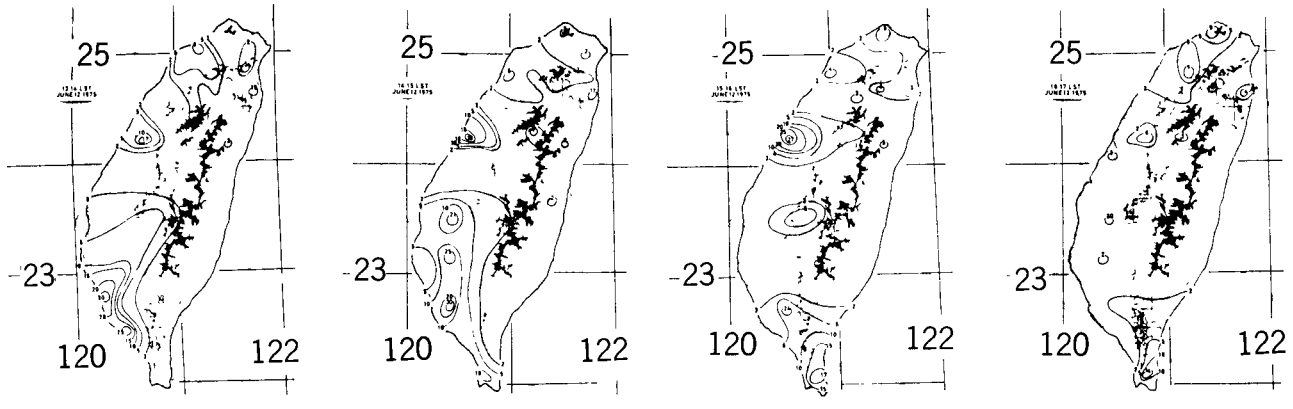

Fig. 18a Fig. 18b Fig 18c Fig 18d

Fig. 18 Hourly rainfall (mm) in Taiwan on June 12, 1975 for (a) 1300-1400 LST, (b) 1400-1500 LST, (c) 1500-1600 LST, (d) 1600-1700 LST.

Hourly rainfall distributions form 1300LST to 1700LST on June 12 are shown in Fig. 18. A local rainfall maximum was again observed near Taichung with hourly amount of 17, 18, 27, and 6 mm during this 4 h period. During the first two hours, rainfall generally occurred over the western plain. The southwestern plain had hourly rainfall greater than 30 mm. This maximum rainfall system tended to move southeastward.

Five areas in Taiwan were defined according to the similar characteristics of rainfall and geographical locations of the surface stations. Twenty one stations of Chinese Central Weather Bureau (see Table 1 and Fig. 19) represent these five areas as follows: (1) N. Area: Anpu (691), Chutzhu (693), Tanshui (690), Taipei (692), Hsinchu (757); (2) C.

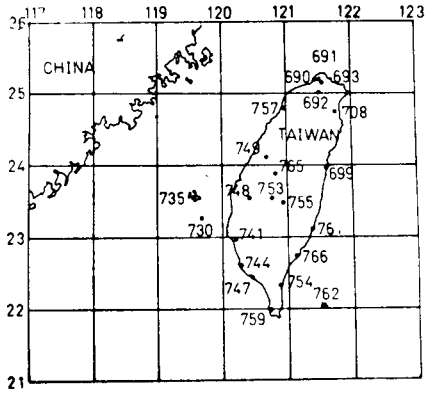

Fig. 19

Fig. 19 Twenty one surface and three radiosonde stations in Taiwan as presented in Table 1.

Table 1 List of 21 surface stations and 1 radiosonde station of Chinese Central Weather Bureau (CCWB) and 2 radiosonde stations of Chinese Air Force (CAF) in Taiwan.

Station Name	number	latitude	longitude	elevation(m)
Anpu	46691	25°11′	121°31′	836 2
Chutzhu	46693	25°10′	121°32′	600.0
Tanshui	46690	25°10′	121°26′	19.0
Taipei	46692	25°02′	121°31′	8 0
(Radiosonde, CWB)				
Hsinchu	46757	24°48′	120°58′	32.8
Taichung	46749	24°09′	120°41′	83.8
Penghu	46735	23°32′	119°33′	9.4
Chiayi	46748	23°30′	120°25′	26 8
Tungchie	46730	23°16′	119°40′	45.5
Tainan	46741	23°00′	120°13′	12.7
Kaoshiung	46744	22°37′	120°16′	29.1
Lanyu	46762	22°02′	121°33′	323.3
Hengchun	46759	22°00′	120°45′	22.3
Jihyuehtan	46765	23°53′	120°51′	1014.8
Alishan	46753	23°31′	120°48′	2406.1
Yushan	46755	23° 29′	120°57′	3850.0
Yilan	46708	24°46′	121°45′	7.4
Hwalien	46699	23°58′	121°37′	17.6
Hsinkang	46761	23°06′	121°22′	36.5
Taitung	46766	22°45′	121°09′	8.9
Tawu	46754	22°21′	120°54′	7.6
Makung	46734	23°50′	119°62′	29.0
(Radiosonde, CAF)				
Tungkong	46747	22°47′	120°47′	3.0
(Radiosonde, CAF)				

Area: Taichung (749), Penghu (735), Chiayi (748), Tungchie (730); (3) S. Area: Tainan (741), Kaoshiung (744), Lanyu (762), Hengchun (759); (4) M. Area: Jihyuehtan (765), Alishan (753), Yushan (755); (5) E. Area: Yilan (708), Hwalien (699), Hsinkang (761), Taitung (766), Tawu (754). Time sections of hourly rainfall averaged over the stations in four areas are shown in Fig. 20. In N Area, continuous rain is observed. Sign of intermittent heavy rain is also indicated. Rainfall intensity increases rather rapidly during the early hours of June 11 and decreases more slowly after June 12. Continuous or intermittent rain is also observed for the other areas. Relative rainfall minimum is observed in C and M Areas on June 13 and 14. Maximum intensity of rainfall over S Area is found from 1200 LST, June 13 to 1200LST June 14. Small amound of rainfall is observed for E Area (not shown).

In order to detect the diurnal variations, the hourly rainfalls averaged over the 6-day period are presented in Fig. 21. Afternoon maximum is suggested for C, and M Areas. A single maximum near noon time is observed for S Area. Patterns of N Area seems to suggest an early morning minimum, although the maximum is not clearly indicated.

Power spectrum analysis of the hourly rainfall averaged over stations in various areas, as shown in Fig. 20, is made and presented in Fig. 22. Rainfall

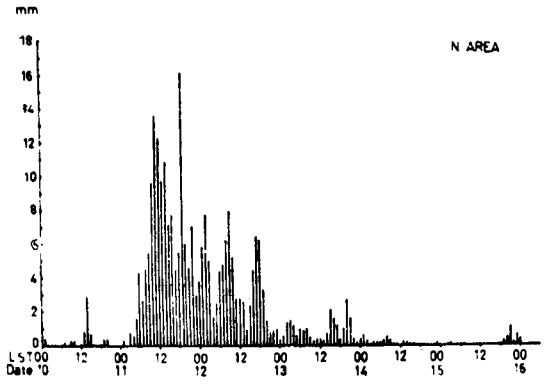

Fig. 20a

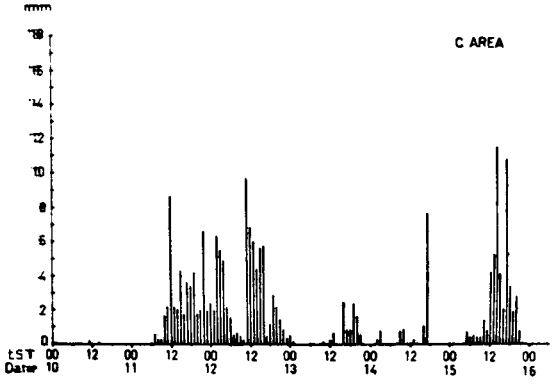

Fig. 20b

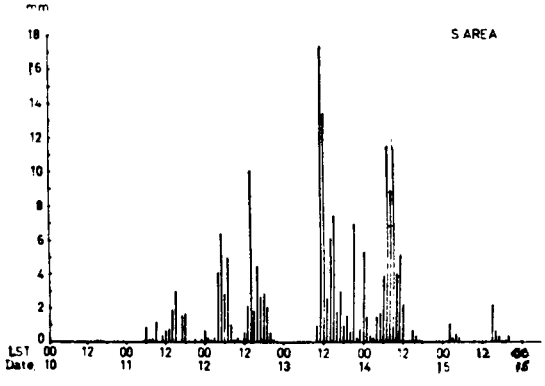

Fig. 20c

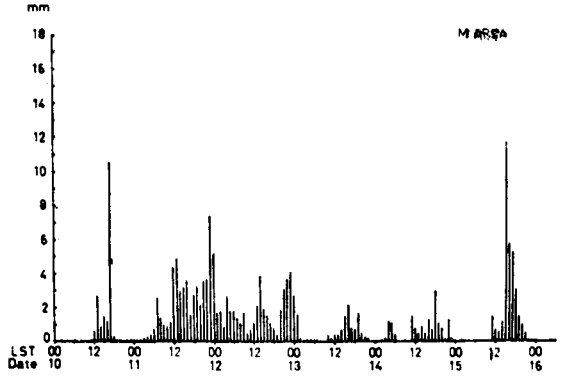

Fig. 20d

Fig. 20 Time sections of area averaged hourly precipitation (mm) in Taiwan for June 10 through 15, 1975 over (a) northern area (N Area), (b) central area (C Area), (c) southern area (S Area), (d) mountain area (M Area).

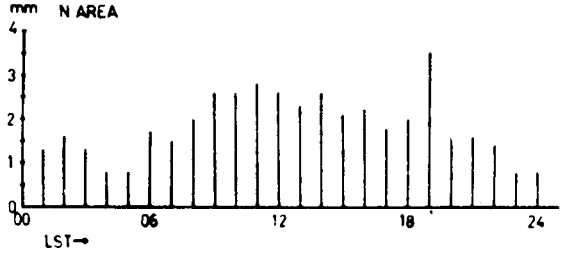

Fig. 21a

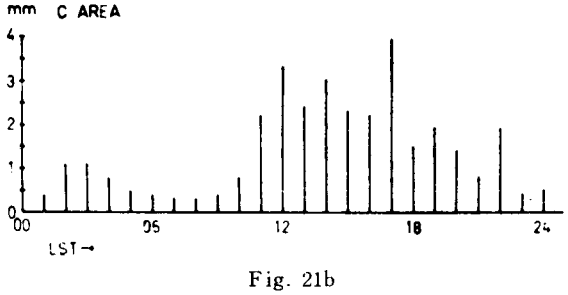

Fig. 21b

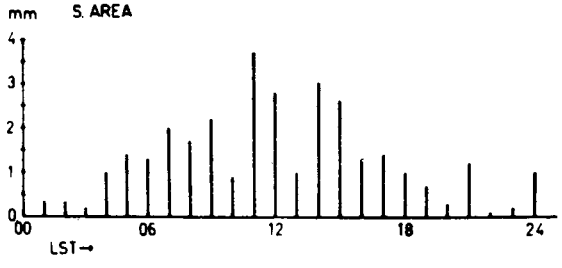

Fig. 21c

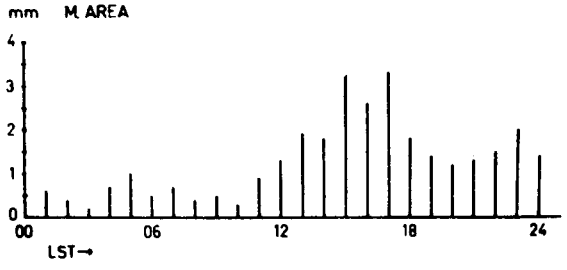

Fig. 21d

Fig. 21 Diurnal variations of area averaged precipitation (mm) during the period of June 10-15, 1975 in Taiwan for (a) N Area, (b) C Area, (c) S Area, (d) M Area.

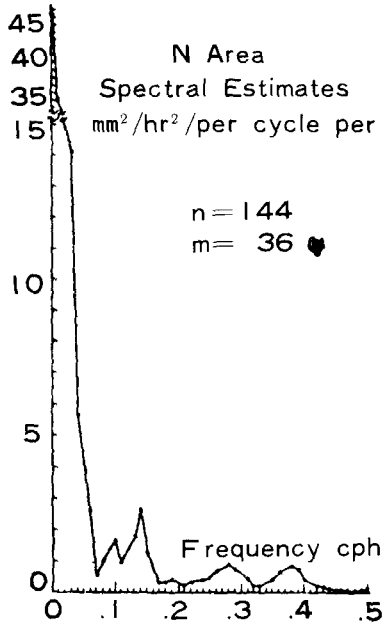

Fig. 22a

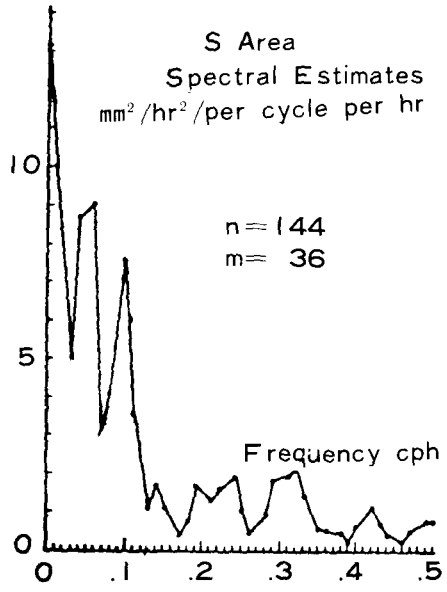

Fig. 22b

Fig 22 Power spectrum of hourly precipitation of a time series of 144 h from June 10 to 15, 1975 for (a) N Area, (b) S Area. Maximum time lag of 36 h is used and the hamming smoothing is applied.

peaks with time periods of 7.1 h, 3.5 h and 2.6 h are found with statistical significance for N Area. Whereas over S Area, spectrum peaks are found at 16.6-25 h, 4.2-5 h, 3.1-3.4 h and 2.4 h. No significant peak is found over C, M and E Areas (not shown)

Since the well-defined spatial and temporal continuity is evidently exhibited in the hourly rainfall patterns (Figs. 17 and 18), contingency index analysis is made in an effort to estimate the wavelength and time periods of mesoscale rain systems. A 3x3 contingency table is constructed by counting the frequency of occurrences of hourly rainfall at stations in northern Taiwan. The selected class intervals are taken arbitrarily as 0, 0.1-2.0 mm and $\geq$2.1 mm. The contingency index (CI) as computed from a 3x3 table can have values from +1 to −0.5 (e.g. Brier and Allen, 1951; Henry, 1974). The CI and distance curves between any two stations are plotted during the case period (Fig. 23). The CI of about 0.35 is found with distance near 25, 60 and 85 km. The CI of 0.35 would indicate that the relationship between hourly rainfall totals of two stations is better than random. This observation suggests that the distance from center to center of the rainstorm would be 25, 60, 85, 110, 145 and 170 km and so on. Assuming the rainstorm moved with a mean speed of 24 km h^{-1} (i. e. 13 knot), approximately the averaged radar echo speed, the corresponding time periods would be 1, 2.5, 3.5, 4.5, 6 and 7.1. h. This observation further substantiates the rainfall peak with time periods of 2.6, 3.5, and 7.1 h found in the spectral analysis for N Area.

Data from a 10-cm meteorological radar of the model WSR-64 at Kaoshiung are examined at 3-h intervals. Two strips of echo amount, AA′ and BB′, taken as approximately parallel to the direction of echo movement are analyzed during the case period in an effort to reveal the wave structure of the radar echoes. Additional strip CC′, is arbitrarily taken to help the analysis. The basic map of these strips and the results are shown in Figs. 25 and 28. The wave structure of radar echoes is clearly indicated by the solid (or dashed) straight lines. The wave period is estimated to be 17 h and the wave speed along AA′ and BB′ is about 5 m s^{-1}. The wavelength is approximately 300 km. The northward propagation of the wave over the Bashi Channel is also suggested.

The southward movement of the maximum center of hourly and 6-hourly rainfall in Taiwan on June 11 as shown in Figs. 15 and 17 are clearly seen in the radar echo reports. These echoes propagates southeastward in the Taiwan Strait. The hourly rainfall maxima on the southwestern and southern Taiwan on June 12 (Fig. 18) are also clearly indicated in the radar echoes propagating from the northwest (Fig. 28). Heavy rainfall in S Area (Fig. 20) from 1000LST to 1700LST, June 13 is due primarily to the intrusion of echo cluster from the Bashi Channel. Rainfall maximum is observed on June 15 in C and M Areas as shown in Fig. 19. Radar echoes responsible for this rainfall maximum apparently propagates into

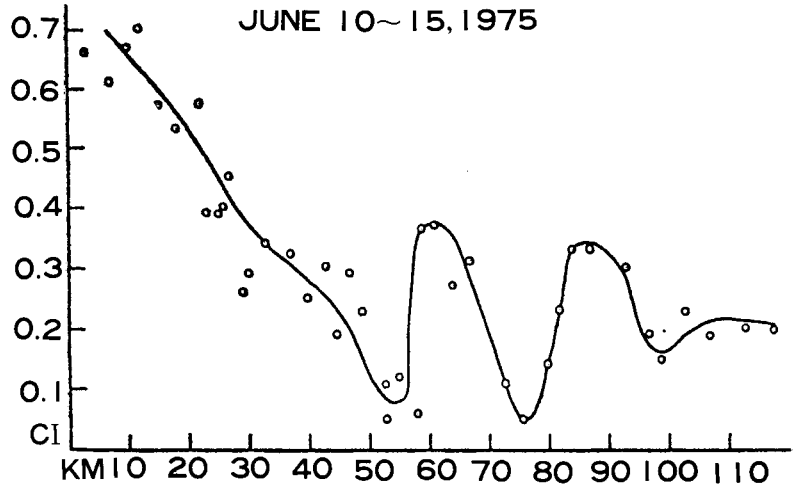

Fig. 23 Contingency index (CI) vs distance for stations in northern Taiwan for June 10-15, 1975.

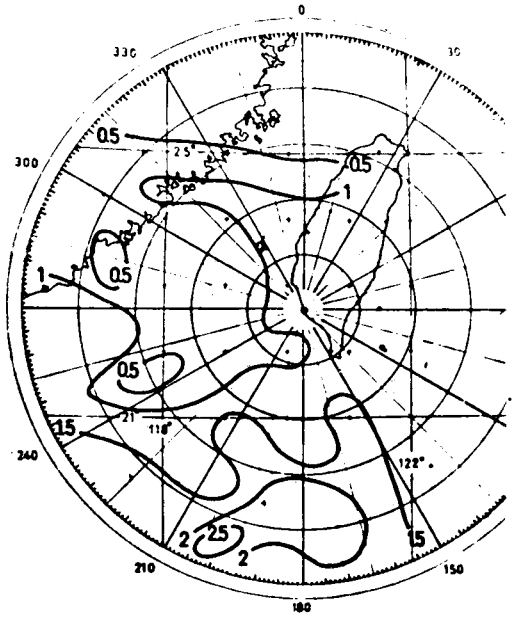

Fig. 24a

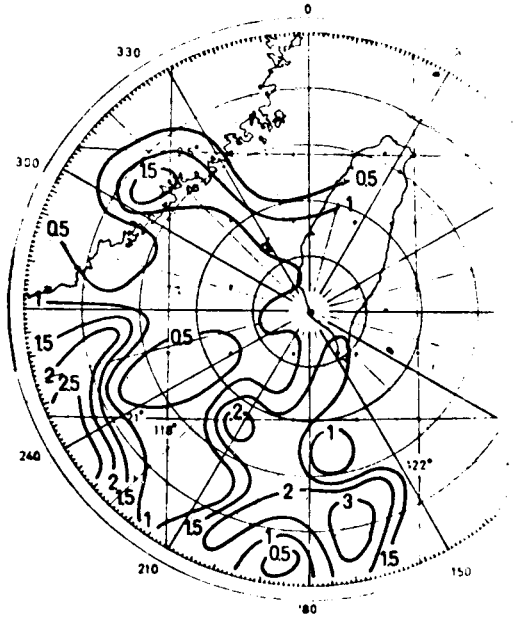

Fig. 24b

Fig. 24 Distributions of (a) relative echo amount, (b) relative standard deviation of echo amount, for June 10-15, 1975.

the area from the south. Topographical effect possibly interacted with the rain system and enhanced the rainfall during this time period. Evidently, the rainfall in Taiwan was due to the organized mesoscale rainfall systems as evidenced by echo clusters which were pre-existing outside the island. Echo clusters moved inland with a southward component on June 11 and 12 but with a northward component on June 13 and 15.

Radar echo amounts for every section bounded by concentric circles at 50 nautical mile interval and azimuth angle at 15 degree interval are estimated at 3-h interval. In order to show the distribution and variation of echo amount as well as to eliminate the effect of attenuation due to distance, time averaged relative eaho amount (REA) and relative standard deviation (RSD) of echo amount are computed. The REA for each section is defined as the value of time averaged section echo amount divided by the value of mean echo amount over all sections at equidistance. Accordingly, the RSD is similarly defined. The procedure used is identical to that by Ninomiya (1974). Note that the value in the area beyond 200 nautical miles are not reliable due to the small amount of echo reports. The small values of REA and RSD are found over the area to the southwest of Taiwan (Fig. 24). Whereas the large values of REA and RSD are observed over the Bashi

Channel and the immediate west of Taiwan. This distribution tends to suggest that the intensity of existing rain system in the Mei-Yu Front was reinforced by local orography as well as by the warm sea surface temperature.

Radar echo amounts are also analyzed in the area bounded by 118°E and 121°E, 20°N and 26°N as shown in Fig. 25. Grid size of one-twelfth degree longitude by one-twelfth degree latitude is used to estimate the echo amount. An east-west strip of four degree longitude contains fourty-eight grids. Each north-south strip in regions X(24°N−26°N), Y(22°N−24°N), Z(20°N−22°N) includes two degree latitude, i. e. twenty-four grids. Time sections of radar echo amount averaged over the east-west strip are shown in Fig. 26 to reveal the north-south mean propagation of the radar echoes. Two axes of maximum echo amount are found in regions X and Y before June 12, 1200GMT. The corresponding mean echo speeds are estimated to be 2.5m s^{-1} and 7.5m s^{-1}. Northward propagatation of maximum echo amount from region Z to Y before 1200GMT, June 13 is also clearly seen and the corresponding speed is about 6.5 m s^{-1}. The maximum echo amount near 0600GMT (1400LST) is evident, especially over regions Y and Z.

Diurnal time sections of six-day mean radar echo for the north-south strip are shown in Figs. 27(a) and 27(b) for the regions Y and Z, respectively. In region Y, a maximum is found near 120°E at

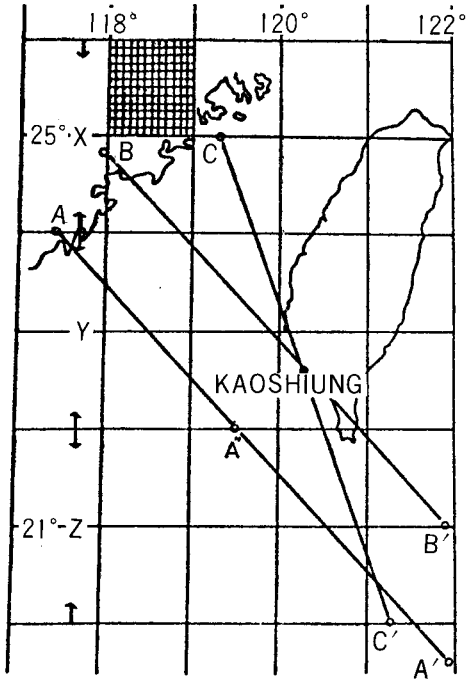

Fig. 25 Basic map for radar echo amount computations in regions X(24°N-26°N), Y(22°N-24°N), and Z(20°N-22°N) bounded by 118°E and 121°E and for radar echo propagation analyses.

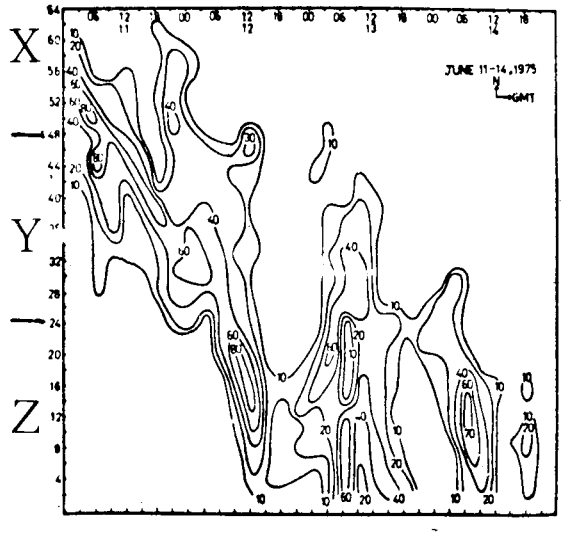

Fig. 26 Time sections of east-west-strip mean radar echo amount (%) between 20°N and 26°N for June 10-15, 1975. Ordinates are indices which indicate the strip latitudes, e. g. 12 is 21°N and 24 is 22° N etc.

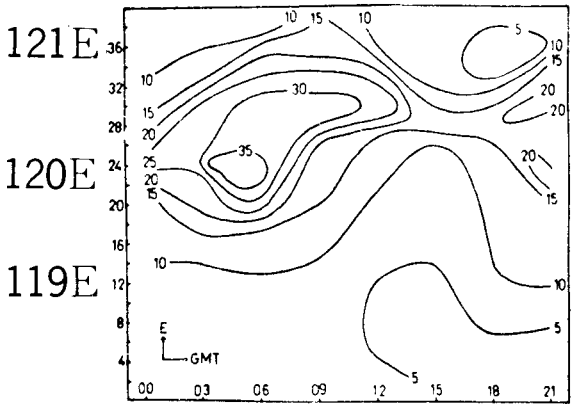

Fig. 27a

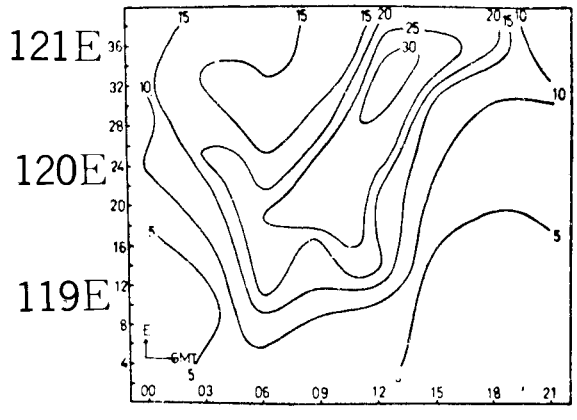

Fig. 27b

Fig. 27 Diurnal variations of radar echo amounts (%) for the north-south-strip in (a) region Y, (b) region Z for June 10-15, 1975.

0600GMT (i.e. 1400LST) and then extends eastward and weakens. In other words, the echo amount reaches a maximum in the vicinity of the coast in the early afternoon and them moves inland and weakens. This reflects the importance of thermal control on the daily rainfall in the area. This echo variation is consistent with the diurnal rainfall variation in central and southern Taiwan with a single maximum near early afternoon (Fig. 21). Over the region Z (Bashi Channel), the maximum echo appears to propagate eastward from 119.5°E near 0600 GMT (1400LST) and reaches a maximum at 121°E near midnight (1600GMT). Care has to be exercised, however, as the echo amount is not adjusted according to the distance to eliminate the attenuation effect.

Winds aloft in the vicinity of Taiwan Strait are analyzed to study their relationships with the echo

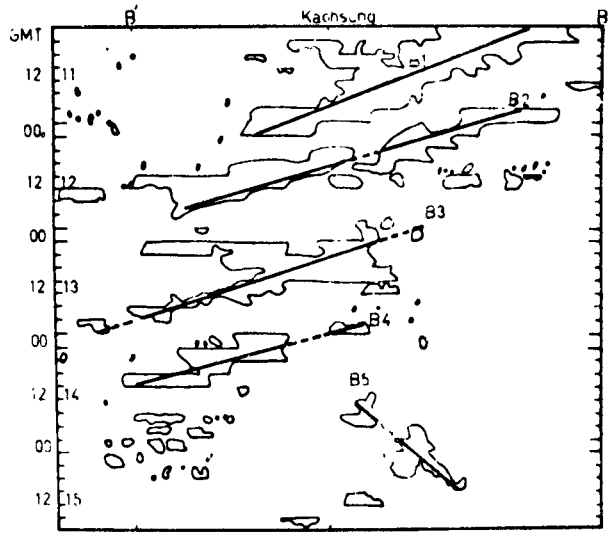

Fig. 28b

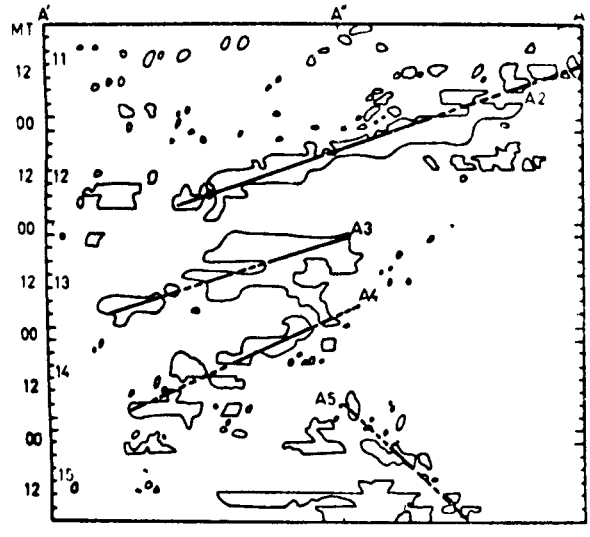

Fig. 28a

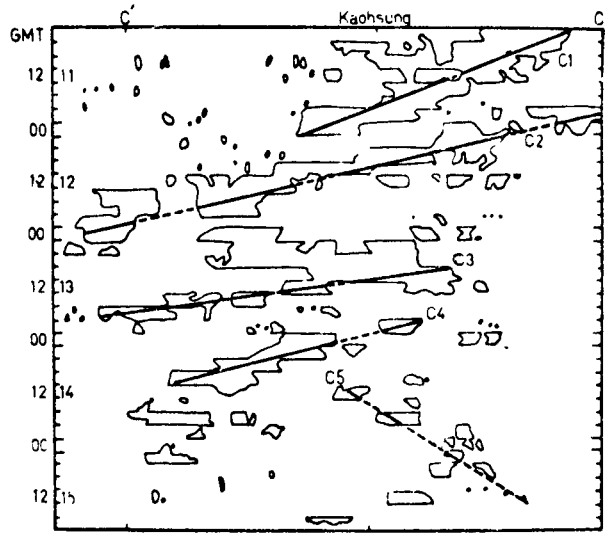

Fig. 28c

Fig. 28 Time sections of echo (light solid line envelops) along (a) AA′, (b) BB′, (c) CC′ as shown in Fig. 25. Echo systems are indicated by heavy solid (or dashed) straight lines and are numbered accordingly.

propagation. Echo clusters are found to move toward right of the mean wind in 850-500 mb layer with an averaging deviation of 25° during the six day period. They also tends to move toward the area of positive moisture advection in the lower troposphere and toward the area of maximum large scale upward motion at 700 mb (Fig. 10). It is synoptically reasonable as moisture supply and upward motion provides favorable conditions for the individual new cells to grow within cluster to the right of mean wind. The movement of echo cluster associated with Mei-Yu Front is, thus, in a sense similar to the movement of large convective clusters in the Mid-West of tne United States (e.g. Newton and Katz, 1958; Newton and Newton, 1959).

Discussion

Observational studies on mesoscale rain systems under various synoptic situations have been one of the major research interests in recent years. Results of detailed analyses on organized mesoscale precipitation patterns in New England tend to suggest that the convective activity serves as a direct mechanism to bring the synoptic scale to saturation favorable for cyclogenesis (Bosart, 1973). Kreitzberg and Brown (1970) used a 10-site mesoscale rawinsonde network coupled with radars and surface observations to study mesoscale weather systems within an occlusion over New England. Their results shows that a subsynoptic core of cold dry air in the middle troposphere ahead

of the surface occlusion serves as a mechanism to suppress the widespread cloudiness and precipitation while to creat the potential instability. The large scale ascending motions then releases the potential instability around this cold core.

Results of this study show that the scale interactions as cited above are also evident and important in the vicinity of Mei-Yu Front. Pre-existing potential instability is realized by the large scale ascent. As a result, the occurrence of convective activity is responsible for the release of latent heat and upward transport of moisture. Thus, the convective activity tends to bring the environment to saturation and leads to a more stable condition by increasing θ_e in the mid-troposphere. To illustrate, let us inspect more closely the structures of moisture and three dimensional winds near a Mei-Yu Front in the vicinity of Taiwan. In N Area, heavy convective rainfall between 11, 0000GMT and 12, 1200GMT is found with potential instability below 600 mb (Figs. 7 and 20a). Maximum instability is found at the beginning of this period while slight instability is observed near the end of strong convective rainfall. Convective precipitation tends to bring the atmosphere to saturation in lower and middle troposphere. Thickness of the unstable layer decreases to the lowest 100 mb as the convective activity diminishes and the low level easterly jet sets in after 12, 1200GMT. The more nearly stratiform steady precipitation is observed after that time. The low level southwesterly jet near 700 mb in the vicinity of Taiwan serves as a mechanism to transport both the moisture and heat to the warm side of Mei-Yu Front and leads to a maximum θ_e at that level (Figs. 6 and 11). Thus, the low level southwesterlies, especially the LLJ, tend to creat the potential instability (see also Figs. 7, 8, and 9). Continued large scale ascents (Fig. 10) then lead to the release of potential instability. As a result, convective precipitation tends to bring the atmosphere to near saturation and the high θ_e in the mid-troposphere. Thus, the large scale ascents release the potential instability, caused mainly by LLJ, through the convective activities. Similar situation is also evident in C and M Areas between 11, 0000GMT and 12, 1200GMT and in S Area between 13, 0000GMT and 14, 0000GMT (Figs. 8, 9, and 20). While the LLJ is found to the warm side of Baiu Front on occasions of prolonged heavy rain in Japan, the downward transfer of horizontal momentum by cumulus convection is called upon to explain the maintenance of the LLJ (Matsumoto et al 1970, 1971). This study, on the other hand, suggests that the pre-existing LLJ is the main mechanism to creat potential instability to the warm side of a Mei-Yu Front and leads to convective precipitations.

The mechanism directly governing the mesoscale rain systems is the release of potential instability by large scale vertical motions in the vicinity of Mei-Yu Front. The convection that is released produces the radar echoes and the cells of heavy precipitation. Surface hourly rainfall discloses that the mesoscale rain systems have the time periods of 2.6, 3.5, and 7.1 h in northern Taiwan. Radar echoes analysis shows that the echo clusters tends to move toward right of the mean wind in 850-500 mb layer with an averaging deviation of 25°. These echo clusters, while moves southeastward in the Taiwan Strait, appears to have a wavelength of 300 km and wave period of 17 h.

As the precipitation in Taiwan is mainly due to the preexisting rain systems during a Mei-Yu regime, the local orography as well as the warm sea surface temperature tends to reinforce its intensity. Diurnal variations of surface rainfall as well as radar echo amounts suggest that the diurnal thermal control might also play a role in regulating the rainfall intensity, especially in central and southern Taiwan.

Forecasting rainfall based on the forecast large scale vertical velocity may fail to identify some important situations of mesoscale rain systems in Mei-Yu season unless a proper way is found of taking into account of the mesoscale systems in both the numerical and synoptic models. Further studies are needed in this aspect to better understand the mesoscale features. While the release of potential instability by large scale ascents is of central importance in the intensification of tropical disturbances and in causing a great amount of precipitation in extratropical cyclones, it is also an important process in causing the heavy convective rainfall in Mei-Yu Front. During the southeastward journey of a Mei-Yu Front, the intensity of relative vorticity tends to conserve while the baroclinicity is weakening. Results of this study bring up some questions about the role of the above-mentioned process as well as the release of latent heat in maintaining the intensity of relative vorticity in a Mei-Yu Front. Future studies will be focused on this aspect.

Acknowledgements

The author wishes to express his sincere appreciation to professor Griffith Wang for reading the manuscript. Thanks are due to Miss Fuh-Mei Chen for typing the manuscript. This paper represents a portion of the results in Mei-Yu Project termed "Synoptic-Dynamic Studies of Mei-Yu in Taiwan". The research was made possible through Grant NSC-65-0202-01(03) from the National Science Council of the Republic of China.

References

1. Bosart, L. F., Detailed analyses of precipitation patterns associated with mesoscale features accompanying United States East Coast cyclogenesis. *Mon. Wea. Rev.*, 101, 1, 1-12. (1973).
2. Brier, G. W. and R. A. Allen, Verifications of weather forecasts. *Compendium of Meteorology*. (T. F. Malone, Ed.), Boston, Amer. Meteor. Soc., pp. 841-848. (1951).
3. Chen, G. T. J., A composite case study of kinematic vertical motion. *Atmos. Sci.*, Meteor Soc. Rep. of China, 3, 87-105. (1976).
4. Henry, W. K., The tropical rainstorm. *Mon. Wea. Rev.*, 102, 10, 717-725. (1974).
5. Kreitzberg, C. W. and H. A. Brown, Mesoscale weather systems within an occlusion. *J. Appl. Meteor.*, 9, 3, 417-432. (1970).
6. Matsumoto, S., S. Yoshizumi and M. Takeuchi, On the structure of the "Baiu Front and the associated intermediate-scale disturbances in the lower atmosphere." *J. Meteor. Soc. Japan*, 48, 6, 479-491. (1970).
7. _____, K. Ninomiya and S. Yoshizumi, Characteristic features of "Baiu" front associated with heavy rainfall. *Ibid*, 49, 4, 267-281. (1971).
8. Newton, C. W. and S. Katz, Movement of large convective rainstorms in relation to winds aloft. *Bull. Amer. Meteor. Soc.*, 39, 129-136. (1958).
9. _____, and H. R. Newton, Dynamical interactions between large convective clouds and environment with vertical shear. *J. Meteor.*, 16, 483-496. (1959).
10. Ninomiya, K., Influence of the sea surface temperature on the stratification of air mass and the cumulus activity over the East China Sea in the Baiu Season. Paper in *Meteor. and Geophys.*, 25, 3, 159-175. (1974).
11. , and T. Akiyama, Medium-scale echo clusters in the Baiu Front as revealed by multi-radar composite echo maps (Part I). *J. Meteor. Soc. Japan*, 50, 6, 558-569. (1972).
12. , Medium-scale echo culsters in the Baiu front as revealed by multi-radar composite echo maps (Part II). Ibid, 51, 2, 108-117. (1973).
13. Nitta, T. and J. Yamamoto, A statistical survey on frequency of the cyclogenesis of the intermediate scale disturbance near Japan, its vicinity and the Southeast Asia. *Ibid*, 50, 3, 234-237. (1972).
14. Ramage C. S., Monsoon Meteorology. Academic Press, N. Y. and London, 296 pp. (1971).

臺灣梅雨期內水氣結構和降水之分析

陳 泰 然

國立臺灣大學大氣科學系

摘 要

本文係針對民國六十四年六月十日至十五日間臺灣地區之梅雨個案，進行其水氣參數及降水系統之分析研究。結果顯示在臺灣海峽上空原已存在之降水系統雷達回波具有週期17小時及波長300公里之特性。這些系統有沿著850—500毫巴平均風偏右25度方向移動之趨勢。當他們移至臺灣上空時，地形效應和溫度日夜變化之熱效應，顯然對決定臺灣地區之降水強度及空間分佈佔有非常重要的角色。結果使得臺灣北部中幅度對流降水系統具有爲時2.6，3.5和7.1小時之週期。

研究結果又顯示低層西南氣流，特別是低層噴射氣流，有在梅雨鋒面南部形成潛在不穩定度的趨勢。而大幅度之連續上升氣流隨即透過對流運動系統來釋放已存的潛在不穩定度。對流運動則產生雷達回波和強烈之降水。